LAWRENCE
LIVERMORE
NATIONAL
LABORATORY

LLNL-TR-650866

Analysis of Composition B Sphere Impact Fragmentation Experiments

H. K. Springer

February 28, 2014

Disclaimer

This work performed under the auspices of the U.S. Department of Energy by Lawrence Livermore National Laboratory under Contract DE-AC52-07NA27344.

Analysis of Composition B Sphere Impact Fragmentation Experiments

H. K. Springer[1], A. I. Atwood[2], K. P. Ford[2]
[1]Lawrence Livermore National Laboratory, Livermore, CA.
[2]Naval Air Warfare Center Weapons Division (NAWCWD), China Lake, CA.

Abstract

Since energetic material fragmentation governs the surface area available for burning and potential escalation to violent reaction modes (e.g., deflagration-to-detonation transition and XDT modes), it is critical that hazard response models accurately capture impact damage response. The objective of this work is to analyze recent Composition B sphere impact experiments conducted by Naval Air Warfare Center Weapons Division (NAWCWD) that probe fragmentation response for impact speeds from 27 to 127 m/s. In those experiments, fragment size distribution was measured by dry sieving damaged samples. A power law relationship was developed for the normalized cumulative fragment number as a function of the normalized fragment mass, $\left({N}/{N_{tot}}\right) = A\left({M_{bin}}/{M_{avg}}\right)^{n}$, across all impact speeds. The power law fits demonstrated good agreement with the experimental data. We also correlated the power law fitting parameters to the impact speed. The power law prefactor, A, obeyed a polynomial relationship while the power law exponent, n, obeyed a linear relationship in impact speed. While this preliminary analysis shows good agreement with Composition B fragmentation data, it was based on experiments over a limited range of impact speeds and a single sample size. Future modeling-based studies are critical to improve our understanding of fragmentation response and to more confidently extrapolate to larger length-scales and higher impact speeds.

Methods

Figure 1 shows a schematic of the 18 mm gas gun used for the Composition B sphere impact fragmentation experiments. Impact speeds varied from 27 to 127 m/s for these experiments. Samples were captured in the catch box and then dry sieved from 3360 to 106 μm using a set of 14 screens to obtain the fragment size distribution for a given impact speed. Composition B spherical samples had a diameter of 18mm, an average density of 1.72 g/cm^3, and a nominal composition of 61wt% RDX, 38wt% TNT, and 1wt% wax. Further details on the NAWCWD Composition B impact fragmentation experiments can be found in [1].

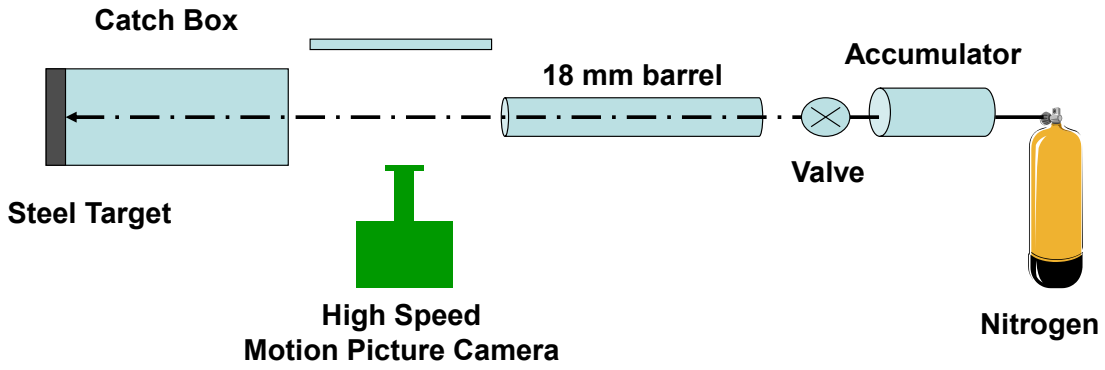

Figure 1. Schematic of the 18 mm gas gun used for the Comb B impact fragmentation experiments [1].

Figure 2 shows an undeformed spherical Composition B sample, as well as damaged samples with an impact speed 27 m/s and 117 m/s. In contrast to the 117 m/s case, several larger fragments with a smaller fraction of "fines" (smaller fragments) are observed in the 27 m/s case. The fines are indications of the brittle nature of Composition B and possibly comminution of the sample during the initial stages of impact with the steel target. Since material fragmentation response is known to be strain-rate dependent and the strain-rate depends on impact velocity, observing smaller more numerous fragments with increased impact speeds is expected.

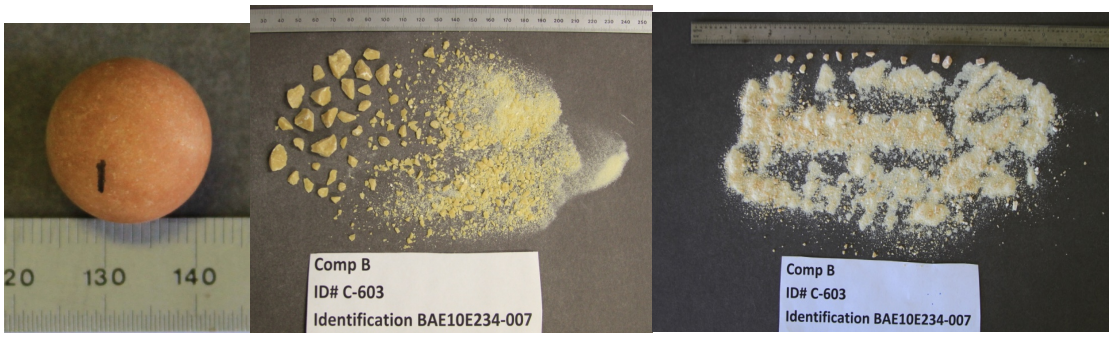

Figure 2. a) Undeformed spherical Composition B sample, b) damaged Composition B sample at 27 m/s, c) damaged Composition B sample at 117 m/s [1].

Results and Analysis

Table 1 shows the results of dry sieving the fragmented Composition B samples with impact speeds from 27 m/s to 127 m/s. For a given impact speed, the sieve mass is the mass collected for a particle sieve size range. The total sieve mass is the mass collected over all sieve sizes and is shown as a percentage of the initial sample mass. The mass recovered in the catch box after impact experiments is also shown. Table 1 data is the basis for all proceeding analyses.

Figure 3 shows a histogram of fragment mass as a function of sieve size for impact speeds of 27 m/s and 117 m/s to further illustrate the change in fragment size distribution with impact speed. The 27 m/s (lowest) case has the largest mass of fragments greater than 3360 μm in size (3.4831 g) but the smallest mass of fragments less than 106 μm in size (0.188 g). In contrast, the 117 m/s case has much less mass in fragments greater than 3360 μm in size (0.2343 g) but more mass in fragments less than 106 μm in size (1.2231 g).

Figure 4 shows the mass recovered in the catch box, as percentage of the initial sample mass, versus the impact speed. The recovered mass decreased with increasing impact speeds. The larger fractions of fines at higher impact speeds may be the cause for low sample recovery at those speeds, i.e., fines are more difficult to recover than large fragments.

Table 1. Mass recovered from dry sieving fragmented Composition B samples.

Sieve Size Range (um)	Sieve Mass (g)	Sieve Mass (g)	Sieve Mass (g)	Sieve Mass (g)	Sieve Mass (g)	Sieve Mass (g)	Sieve Mass (g)	Sieve Mass (g)
>3360	3.4831	2.4512	2.1338	1.1326	1.7008	1.3057	0.8178	0.9889
3360-1000	0.8031	1.3368	1.3461	1.7699	1.2548	1.2878	1.7013	1.6389
1000-840	0.0683	0.0726	0.3157	0.1105	0.1059	0.1602	0.1277	0.1162
840-590	0.1077	0.1841	0.0959	0.2475	0.2363	0.2575	0.2564	0.2336
590-500	0.0516	0.0821	0.0023	0.1154	0.133	0.1249	0.1293	0.1318
500-420	0.0476	0.0758	0.0972	0.1029	0.1121	0.1118	0.1069	0.1178
420-355	0.0566	0.1172	0.1384	0.1502	0.1717	0.1544	0.1894	0.1694
355-250	0.0918	0.1362	0.1987	0.2151	0.2145	0.227	0.212	0.24
250-212	0.0524	0.0732	0.1037	0.1225	0.1202	0.1289	0.1368	0.153
212-180	0.0367	0.0579	0.067	0.0824	0.0871	0.0885	0.0902	0.1029
180-150	0.0446	0.0801	0.1055	0.1128	0.1324	0.1426	0.1796	0.1445
150-125	0.048	0.0791	0.1029	0.114	0.1257	0.1286	0.1217	0.1755
125-106	0.0367	0.0636	0.0928	0.1017	0.1194	0.1162	0.175	0.0969
<106	0.188	0.1932	0.2859	0.4221	0.462	0.4293	0.5855	0.6905
Total Sieve Mass (g)	5.1162	5.0031	5.0859	4.7996	4.9759	4.6634	4.8296	4.9999
Mass Recovered in Catch Box (g)	5.1141	5.0368	5.1504	4.8518	5.0364	4.6999	4.8798	5.0477
Initial Sample Mass (g)	5.2694	5.2635	5.2691	5.268	5.2656	5.2386	5.2647	5.2742
%Initial Sample Mass in Sieves	97.1	95.1	96.5	91.1	94.5	89.0	91.7	94.8
%Initial Sample Mass in Catch Box	97.1	95.7	97.7	92.1	95.6	89.7	92.7	95.7
Impact Speed (m/s)	27.1	38.4	44.8	53.3	57.6	61.0	69.2	70.7
Sieve Size Range (um)	Sieve Mass (g)	Sieve Mass (g)	Sieve Mass (g)	Sieve Mass (g)	Sieve Mass (g)	Sieve Mass (g)	Sieve Mass (g)	Sieve Mass (g)
>3360	0.8236	0.803	0.9919	0.5101	0.7459	0.5177	0.4037	0.41
3360-1000	1.6602	1.3495	1.1947	1.4166	1.3308	1.2533	1.3155	1.277
1000-840	0.1163	0.1166	0.1201	0.1086	0.1246	0.1098	0.1021	0.0972
840-590	0.2608	0.2427	0.2438	0.2376	0.241	0.2702	0.2529	0.2485
590-500	0.1184	0.126	0.1135	0.1221	0.1297	0.1269	0.1341	0.1254
500-420	0.1142	0.1171	0.1223	0.1217	0.1213	0.1394	0.1149	0.1255
420-355	0.1741	0.1744	0.1826	0.1795	0.1713	0.2156	0.1908	0.1795
355-250	0.2597	0.2549	0.2491	0.2884	0.2604	0.2889	0.2733	0.2749
250-212	0.1437	0.1582	0.2406	0.1651	0.1506	0.1755	0.1627	0.1575
212-180	0.1207	0.1107	0.0889	0.1098	0.1208	0.0884	0.1168	0.1477
180-150	0.128	0.1403	0.1136	0.1743	0.1416	0.164	0.1504	0.1378
150-125	0.1516	0.1857	0.1138	0.1807	0.1722	0.1902	0.1923	0.1922
125-106	0.1304	0.2212	0.1742	0.1932	0.1638	0.2388	0.1802	0.2232
<106	0.7525	0.7694	0.7846	0.9833	0.9987	0.9134	1.1035	1.1417
Total Sieve Mass (g)	4.9542	4.7697	4.7337	4.791	4.8727	4.6921	4.6932	4.7381
Mass Recovered in Catch Box (g)	5.0013	4.8395	4.8349	4.8260	4.9392	4.7363	4.7546	4.8111
Initial Sample Mass (g)	5.2676	5.252	5.2628	5.2654	5.2696	5.2673	5.2715	5.2594
%Initial Sample Mass in Sieves	94.1	90.8	89.9	91.0	92.5	89.1	89.0	90.1
%Initial Sample Mass in Catch Box	94.9	92.1	91.9	91.7	93.7	89.9	90.2	91.5
Impact Speed (m/s)	74.4	82.3	84.7	86.9	92.4	95.4	98.1	101.5
Sieve Size Range (um)	Sieve Mass (g)	Sieve Mass (g)	Sieve Mass (g)	Sieve Mass (g)	Sieve Mass (g)	Sieve Mass (g)	Sieve Mass (g)	
>3360	0.4621	0.3375	0.3789	0.3159	0.2343	0.2611	0.1996	
3360-1000	1.0738	1.174	1.2186	1.115	1.1034	0.9937	1.0175	
1000-840	0.0906	0.1111	0.1201	0.0999	0.1088	0.065	0.0976	
840-590	0.2122	0.2954	0.268	0.2476	0.2311	0.1911	0.2189	
590-500	0.1124	0.1382	0.13	0.1242	0.1275	0.1084	0.1272	
500-420	0.1259	0.1268	0.1311	0.124	0.117	0.1222	0.1244	
420-355	0.1866	0.211	0.1924	0.1957	0.2056	0.155	0.1758	
355-250	0.2705	0.2672	0.2772	0.2734	0.2796	0.2597	0.2935	
250-212	0.171	0.1912	0.1723	0.1538	0.1725	0.7124	0.1841	
212-180	0.0905	0.0852	0.1133	0.1407	0.1233	0.0422	0.1178	
180-150	0.2017	0.1931	0.1483	0.1425	0.1713	0.1364	0.1687	
150-125	0.1547	0.1805	0.1774	0.198	0.1919	0.1227	0.22	
125-106	0.1945	0.2045	0.2062	0.2501	0.2438	0.7549	0.694	
<106	0.8377	1.0621	0.9525	1.1688	1.2231	0.416	0.8465	
Total Sieve Mass (g)	4.1842	4.5778	4.4863	4.5496	4.5332	4.3408	4.4856	
Mass Recovered in Catch Box (g)	4.2423	4.6073	4.5454	4.5912	4.5793	4.4991	4.5305	
Initial Sample Mass (g)	5.27	5.2684	5.2634	5.2549	5.2580	5.2572	5.2609	
%Initial Sample Mass in Sieves	79.4	86.9	85.2	86.6	86.2	82.6	85.3	
%Initial Sample Mass in Catch Box	80.5	87.5	86.4	87.4	87.1	85.6	86.1	
Impact Speed (m/s)	105.2	105.2	105.2	112.8	117.3	121.9	127.1	

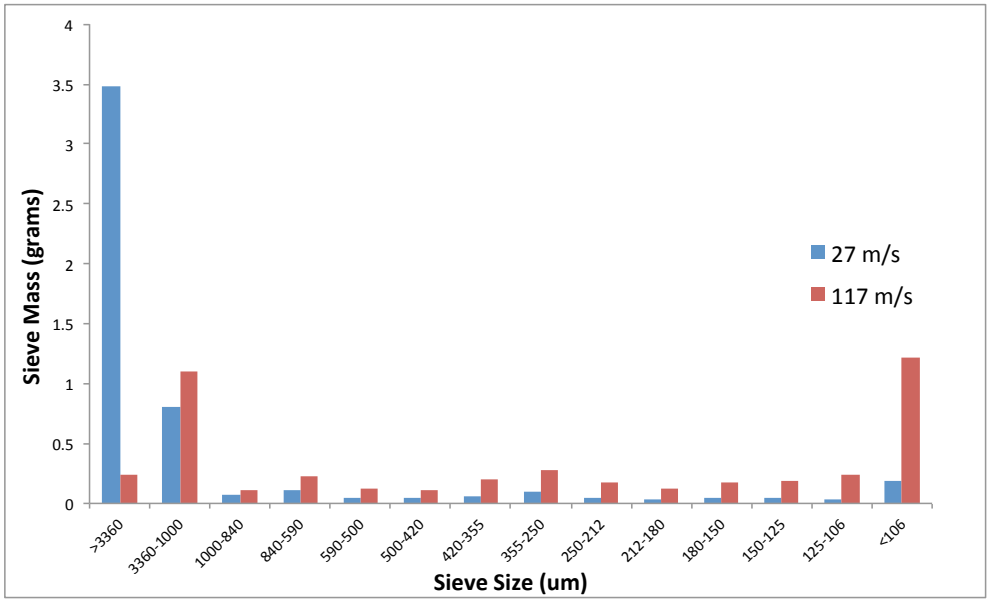

Figure 3. Histogram of fragment mass as a function of sieve size for lower (27 m/s) and upper bound (117 m/s) impact speeds.

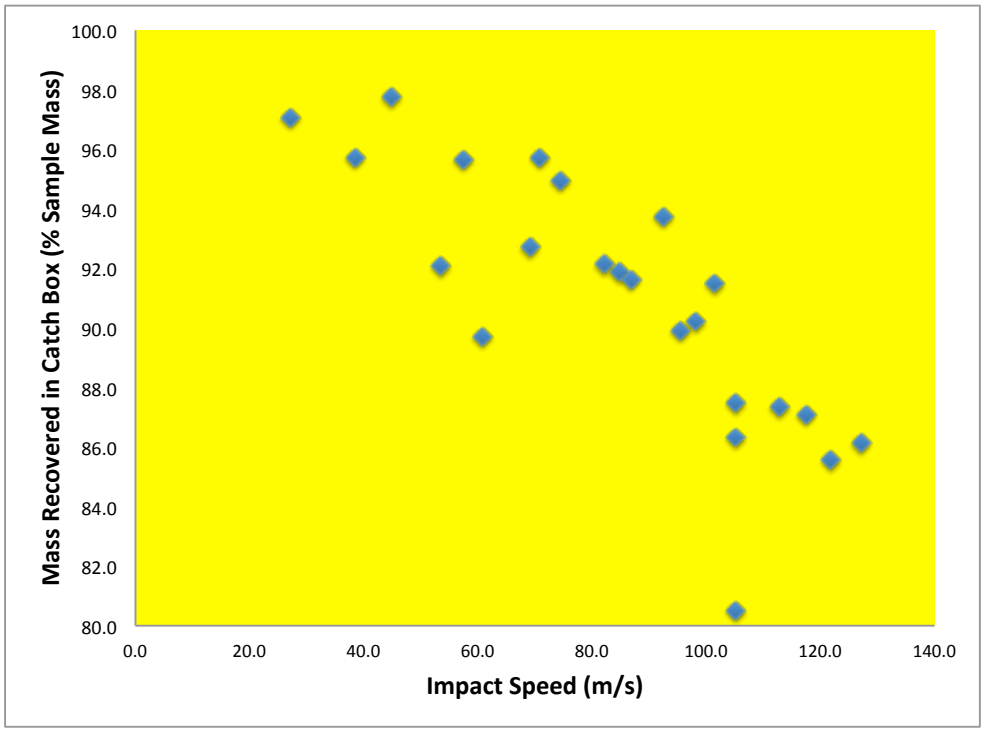

Figure 4. Mass recovered in catch box (% sample mass) versus impact speed.

Based on the measurements in Table 1, we developed a relationship between the normalized cumulative fragment number (N/N_{tot}) and the normalized fragment mass (M_{bin}/M_{avg}). To obtain these quantities, we first calculate a bin size, D_{bin}, by taking the average of the sieve size range, e.g., D_{bin} = 920 μm for 840 to 1000 μm range. For the largest (3360 μm) and smallest (106 μm) bins, we simply use the sieve size for D_{bin}. Based on D_{bin} and the Composition B density (1.72 g/cm^3), we then calculate the bin mass, M_{bin}. We then calculated the overall average size, D_{avg}, based on a mass-fraction weighted average over all the size bins, $D_{avg} = \sum_{i=1}^{N_{bins}} D_{bin,i} mf_i$, where $D_{bin,i}$ is the size, mf_i is the mass fraction of the *ith* bin (N_{bins} = 14), and the mass fraction is the mass recovered in each bin divided by the total recovered mass. An average mass, M_{avg}, was then calculated directly from D_{avg} and the material density. For these calculations, we adjusted the recovered mass in the smallest bin (106 μm) by adding the unrecovered sample mass, i.e., the portion of sample mass not recovered from the catch box ($m_{sample} - m_{recovered}$). This assumption was based on the observation that more mass was lost at higher impact speeds, where a larger fraction of smaller fragments are present, and the practical consideration that the smallest fragments are most difficult to recover. To obtain the number of fragments in each bin, N, we divided (adjusted) recovered mass in each bin by M_{bin}. N_{tot} was simply the sum of the fragments over all the bins.

Figure 5 shows N/N_{tot} as a function of M_{bin}/M_{avg} for impact speeds of 27 m/s and117 m/s. A power law relationship was used to fit this relationship,

$$\left(N/N_{tot}\right) = A\left(M_{bin}/M_{avg}\right)^n$$

where *A* and *n* are the power law fit parameters that are unique for each impact speed case. If the term M_{bin}/M_{avg} is replaced by D_{bin}/D_{avg}, the power law prefactor is identical and the exponent is simply 3*n* since M_{bin} and M_{avg} were calculated from D^3_{bin} and D^3_{avg}, respectively.

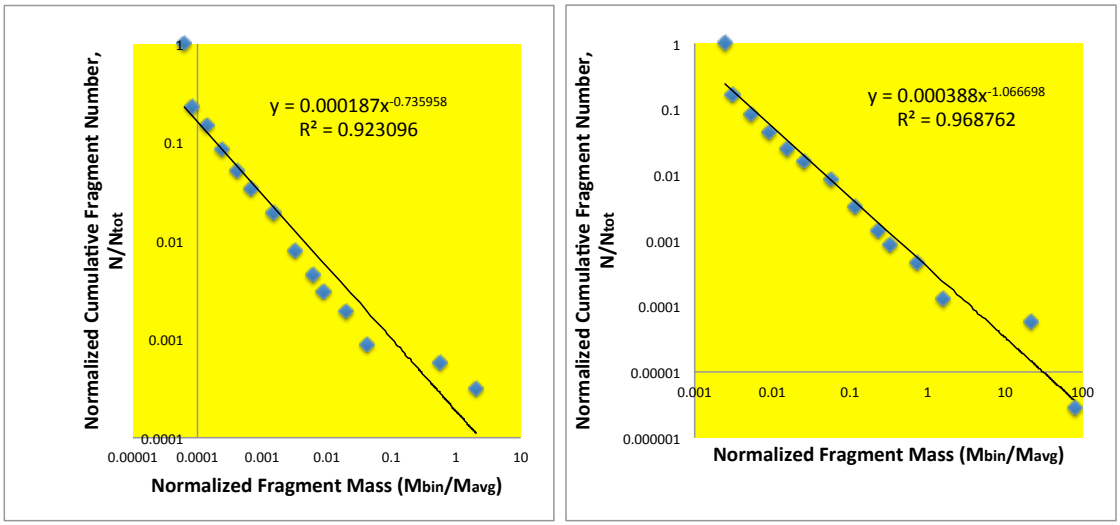

Figure 5. Normalized cumulative fragment number (N/N_{tot}) as a function of normalized fragment mass (M_{bin}/M_{avg}) for impact speeds of 27 m/s and 117 ft/s.

Table 2 summarizes the power law fit parameters for all samples, including the fit correlation (R^2). Good correlation was observed for most of the samples with 22 of 23 samples having $0.95 < R^2 < 0.97$ and a single sample had a lower correlation that still exceeded 0.9.

Figure 6 shows a preliminary attempt to correlate the fragmentation response, i.e., power law fit parameters, with the sample impact speed. The power law prefactor, *A*, obeyed a polynomial relationship while the power law exponent, *n*, obeyed a linear relationship in impact speed.

While this preliminary analysis shows good agreement with Composition B fragmentation data, it was based on experiments over a limited range of impact speeds and a single sample size. Future modeling-based studies are critical to improve our understanding of fragmentation response and to more confidently extrapolate to larger length-scales and higher impact speeds.

Table 2. Power law fit parameters for each sample impact speeds.

Impact Speed (m/s)	*A*	*n*	Fit Correlation
27.1	1.87E-04	-0.736	0.923
38.4	1.85E-04	-0.797	0.948
44.8	0.000199	-0.825	0.951
53.3	1.85E-04	-0.884	0.961
57.6	1.72E-04	-0.88	0.962
61.0	1.79E-04	-0.9	0.964
69.2	2.02E-04	-0.931	0.966
70.7	1.98E-04	-0.921	0.966
74.4	2.06E-04	-0.932	0.966
82.3	2.05E-04	-0.962	0.965
84.7	1.90E-04	-0.947	0.964
86.9	2.41E-04	-0.996	0.967
92.4	2.12E-04	-0.964	0.966
95.4	2.76E-04	-0.999	0.969
98.1	2.73E-04	-1.013	0.967
101.5	2.76E-04	-1.02	0.967
105.2	2.84E-04	-1.022	0.964
105.2	3.40E-04	-1.032	0.97
105.2	3.11E-04	-1.016	0.969
112.8	3.48E-04	-1.042	0.968
117.3	3.88E-04	-1.067	0.969
121.9	4.87E-04	-1.112	0.968
127.1	4.65E-04	-1.103	0.969

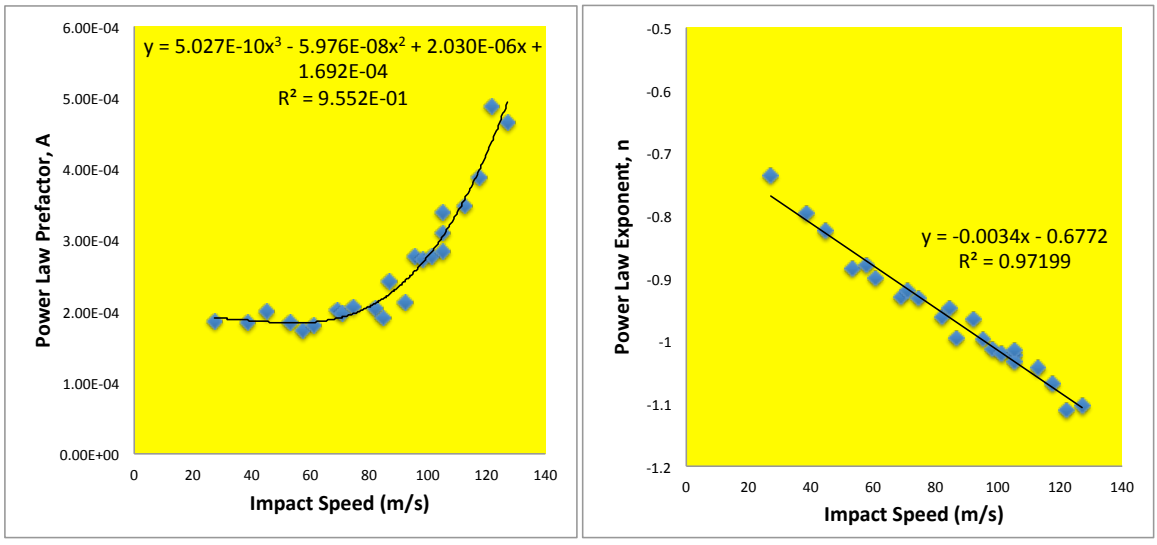

Figure 6. Correlation of power law parameters, *A* and *n*, with sample impact speed. Fits are shown on the figures.

Acknowledgements
This work was performed under the auspices of the U.S. Department of Energy by Lawrence Livermore National Laboratory under Contract DE-AC52-07NA27344. Naval Air Warfare Center Weapons Division (NAWCWD) work was performed for LLNL under Interagency Agreement Number DENA0002268.

References
[1] Atwood A I, Ford K P, et al. Composition B Damage Studies, Naval Air Warfare Center Weapons Division (NAWCWD) TM8740.